



## NUMERICAL MODELING OF POROUS CERAMICS MICROSTRUCTURE

*Danuta Miedzińska*

Department of Mechanics and Applied Computer Science  
Faculty of Mechanical Engineering  
Military University of Technology in Warsaw

Received 22 May 2018, accepted 13 December 2018, available online 14 January 2019.

**Key words:** porous ceramics, finite element method, microstructure

### Abstract

The presented research is directed to the porous ceramics microstructural behaviour assessment with the use of numerical methods. Such new material can be used for thermal insulation, filters, bio-scaffolds for tissue engineering, and preforms for composite fabrication. One of the newest and most interesting applications, considered in this work, is a usage of those materials for production of proppants for hydraulic fracturing of shale rocks. The hydraulic fracturing is a method of gas recovery from unconventional reservoirs. A large amount of fracturing fluid mixed with proppant (small particles of sand or ceramics) is pumped into the wellbore and its pressure causes the rock cracking and gas release. After fracturing the fluid is removed from the developed cracks leaving the proppant supporting the fracture. In the paper the grain porous ceramics which is used for proppant particles preparation was studied. The influence of grains distribution on the porous ceramics mechanical behaviour during compression was simulated with the use of finite element method.

### Introduction – aim of research

Porous ceramics is a group of new and very interesting materials. It can be used for thermal insulation, filters, bio-scaffolds for tissue engineering, and preforms for composite fabrication (HAMMEL et al. 2014).

---

Correspondence: Danuta Miedzińska, Katedra Mechaniki i Informatyki Stosowanej, Wydział Mechaniczny, Wojskowa Akademia Techniczna, ul. Gen. Witolda Urbanowicza 2, 00-908 Warszawa, phone: +48 261 83 7867, e-mail: danuta.miedzinska@wat.edu.pl

Porous structure of ceramics can be prepared through many processing techniques. One technique is to simply sinter coarse powders or partially sinter a green ceramic to hinder full densification (HAMMEL et al. 2014). Other traditional methods of fabricating porous ceramics can be divided into three basic processing techniques: replica; sacrificial template; and direct foaming as seen in Figure 1 (STUDART et al. 2006). The development process influences the microstructure of the material, what was presented in Figure 2.

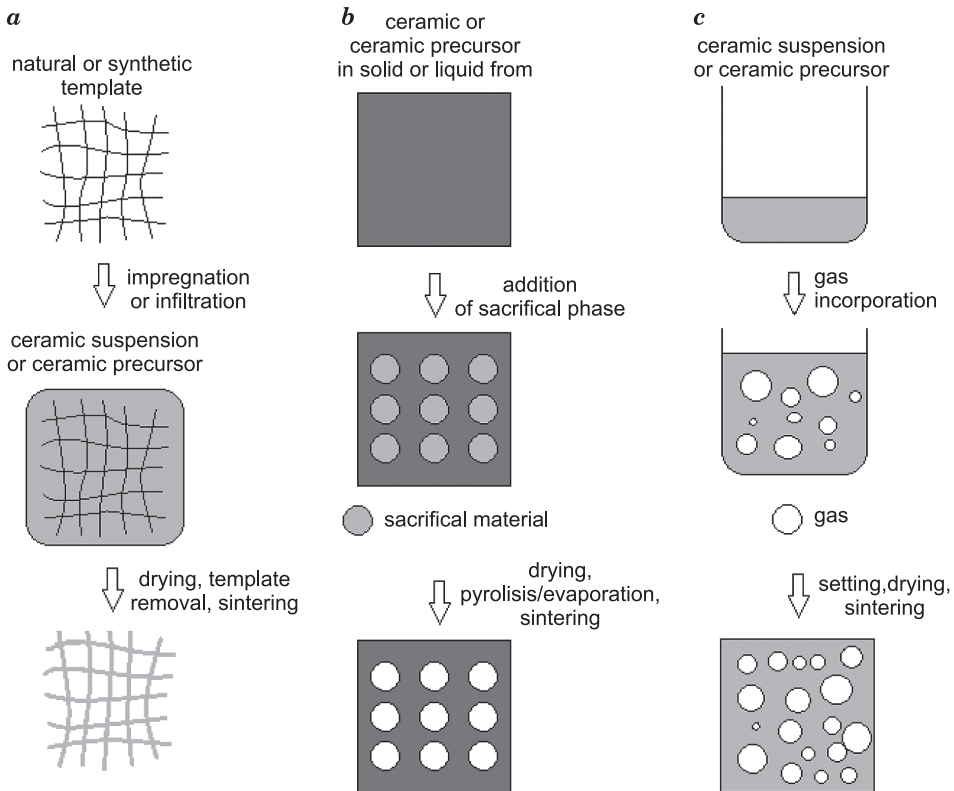


Fig. 1. Typical processing methods for the production of porous ceramics: *a* – replica technique, *b* – sacrificial template technique, *c* – direct foaming technique  
 Source: after STUDART et al. (2006).

One of the newest and most interesting applications is a usage of those materials for production of proppants for hydraulic fracturing of shale rocks (PETTY 2010, MURPHY 2013). The hydraulic fracturing is a method of gas recovery from unconventional reservoirs. A large amount of fracturing fluid (water or CO<sub>2</sub>) (MIEDZIŃSKA et al. 2013) mixed with proppant (small particles

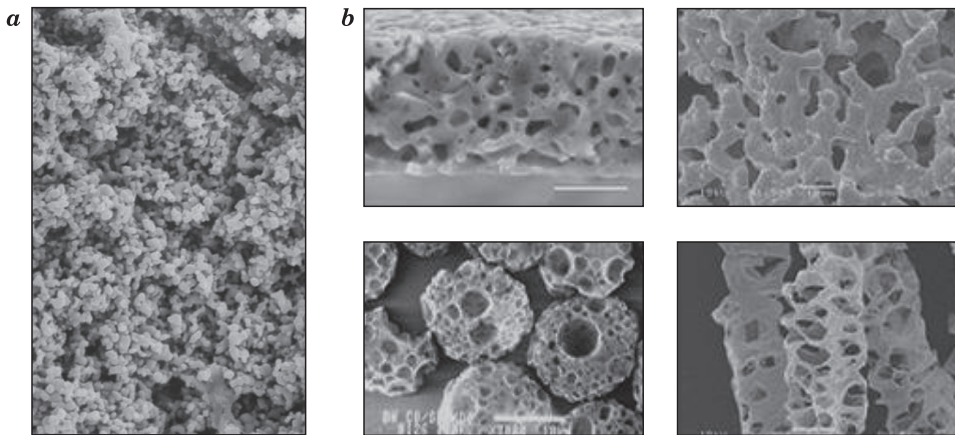


Fig. 2. Porous ceramics microstructure: *a* – grain structure made by sintering, *b* – structure made by replication

Source: *a* – after KALITA et al. (2003), *b* – after WALSH et al. (2005).

of natural sand or ceramics) is pumped into the wellbore and its pressure causes the rock cracking and gas release. After fracturing the fluid is removed from the developed cracks leaving the proppant supporting the fracture (LO et al. 2002), what was shown in Figure 3.

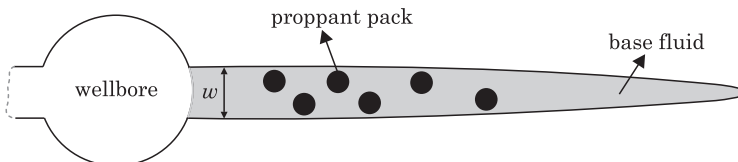


Fig. 3. Crack developed with hydraulic fracturing filled with fluid mixed with proppant

So it is obvious that the proppant should be characterized with high compressive strength but must achieve the highest permeability of the crack. The most often used proppants are natural sands and solid ceramic spheres (KNEZ et al. 2013). The newest solution is the proppant made of cellular ceramics (WEAVER et al. 2007). The example of such structure was shown in Figure 4. Such solution can improve the crack permeability but only in case of assuring the proper strength.

In the paper the main interest is directed to the grain porous ceramics which is used for proppant particles preparation. The numerical modelling of idealized microstructure of such material was presented to study the influence of grains distribution on the porous ceramics mechanical behaviour.

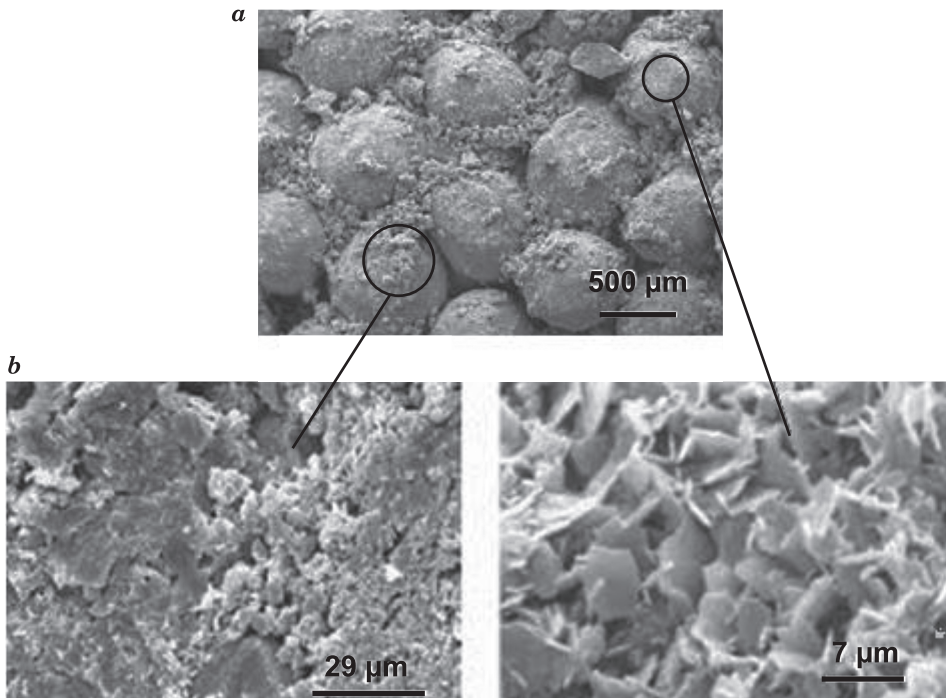


Fig. 4. Porous ceramic proppant: *a* – proppant spheres, *b* – magnitude of porous structure of proppant sphere

Source: after WEAVER et al. (2007).

## Research methodology – numerical models and analyses description

The research was carried out using finite element method. LS Dyna computer code for dynamic analyses were used. Explicit time integration – central difference scheme was applied. This method assesses the linear change in acceleration. It was developed on the base of the single degree of freedom damped system, where forces acting on mass  $m$  are:  $f_s$  – elastic force,  $f_I$  – inertia force,  $f_D$  – damping forces,  $p(t)$  – external forces (HALLQUIST 2016).

The equations of equilibrium are obtained from d’Alambert’s principle:

$$f_I + f_D + f_{\text{int}} = p(t) \quad (1)$$

where:

$$f_I = m\ddot{u}; \quad \ddot{u} = \frac{d^2u}{dt^2} \quad - \text{acceleration,}$$

$$\begin{aligned}
 f_D &= c\dot{u}; & \dot{u} &= \frac{du}{dt} & \text{- velocity} \\
 f_{\text{int}} &= ku; & u & & \text{- displacement.}
 \end{aligned}$$

In the above equations  $c$  is the damping coefficient, and  $k$  is the linear stiffness.

The equations of motion for linear behaviour lead to linear ordinary differential equation:

$$m\ddot{u} + c\dot{u} + ku = p(t) \tag{3}$$

but for the nonlinear case the internal force varies as a nonlinear function of the displacement, leading to the nonlinear formula:

$$m\ddot{u} + c\dot{u} + f_{\text{int}}(u) = p(t) \tag{4}$$

Analytical solutions of linear ordinary differential equations are available, so instead one consider the dynamic response of linear system subjected to harmonic loading. Some commonly used terms can be defined as follows:

$$\begin{aligned}
 p(t) &= p_0 \sin \omega t & \text{- harmonic loading,} \\
 \omega &= \sqrt{\frac{k}{m}} & \text{- circular frequency for single degree of freedom,} \\
 f &= \frac{\omega}{2\pi} = \frac{1}{T} & \text{- natural frequency, } T \text{- period,} \\
 \xi &= \frac{c}{c_{cr}} = \frac{c}{2m\omega} & \text{- damping ratio,} \\
 \omega_0 &= \omega \sqrt{1 - \xi^2} & \text{- damped vibration frequency,} \\
 \beta &= \frac{\bar{\omega}}{\omega} & \text{- applied load frequency.}
 \end{aligned}
 \tag{5}$$

The closed form solution can be defined as:

$$u(t) = u_0 \cos \omega t + \frac{\dot{u}_0}{\omega} \sin \omega t + \frac{p_0}{k} \frac{1}{1 - \beta^2} (\sin \bar{\omega} t - \beta \sin \omega t) \tag{6}$$

with the initial conditions: initial displacement  $u_0$ , initial velocity  $\dot{u}_0$  and static displacement  $\frac{p_0}{k}$ .

For nonlinear problems, only numerical solutions are possible. In the problem described in the paper the explicit central difference scheme, built in LS Dyna, were applied to integrate the equations of motions.

To describe the central difference method the semi-discrete equations of motion at time  $n$  are defined as:

$$Ma^n = P^n - F^n + H^n \quad (7)$$

where  $M$  is the diagonal mass matrix,  $P^n$  accounts for external and body force loads,  $F^n$  is the stress divergence vector and  $H^n$  is the hourglass resistance. To advance to time  $t^{n+1}$ , the central difference time integration is used in the following form:

$$a^n = M^{-1}(P^n - F^n + H^n) \quad (8)$$

$$v^{n+\frac{1}{2}} = v^{n-\frac{1}{2}} + a^n \Delta t^n \quad (9)$$

$$u^{n+1} = u^n + v^{n+\frac{1}{2}} \Delta t^{n+\frac{1}{2}} \quad (10)$$

where:

$$\Delta t^{n+\frac{1}{2}} = \frac{\Delta t^n + \Delta t^{n+1}}{2} \quad (11)$$

and  $v$  and  $u$  are the global nodal velocity and displacement vectors, respectively. The geometry can be updated by adding the displacement increments to the initial geometry:

$$x^{n+1} = x^0 + u^{n+1} \quad (12)$$

The modelling of porous ceramics can be found in literature. In DOLTINIS and DATTKKE (2001) a numerical model for microcrack formation and damage evolution in brittle porous solids under internal fluid pressure was presented. In SHCHUROVA (2016), for the purpose of universality, ceramics grains and pores were modelled as six-sided subareas. In SADOWSKI and SAMBORSKI (2003) a mesomechanical modelling of porous polycrystalline ceramics subjected to different kinds of loading was presented.

Four types of geometry were used to simulate the grains distribution in porous ceramics microstructure, called **u1**, **u2**, **u3** and **u4**. The proposed models were designed to consider the various types of dense packing of sphere shaped grains in idealistic structure. Model **u1** and **u2** were built of 9 spheres packed regularly and hexagonally respectively (like in crystallographic net). Model **u3** was a coupling of model **u1** and **u2**, in which spheres in two bottom rows were distributed regularly and in two top rows – hexagonally. Model **u4** was a modification of model **u1** based on addition of smaller spheres in free spaces between existing ones, such as they are tangent to each other and allow to fill the space in more dense way. Those applied distributions resulted in different porosities and dimensions of the models what influenced the results presentation in relative manner. The models were presented in Figure 5.

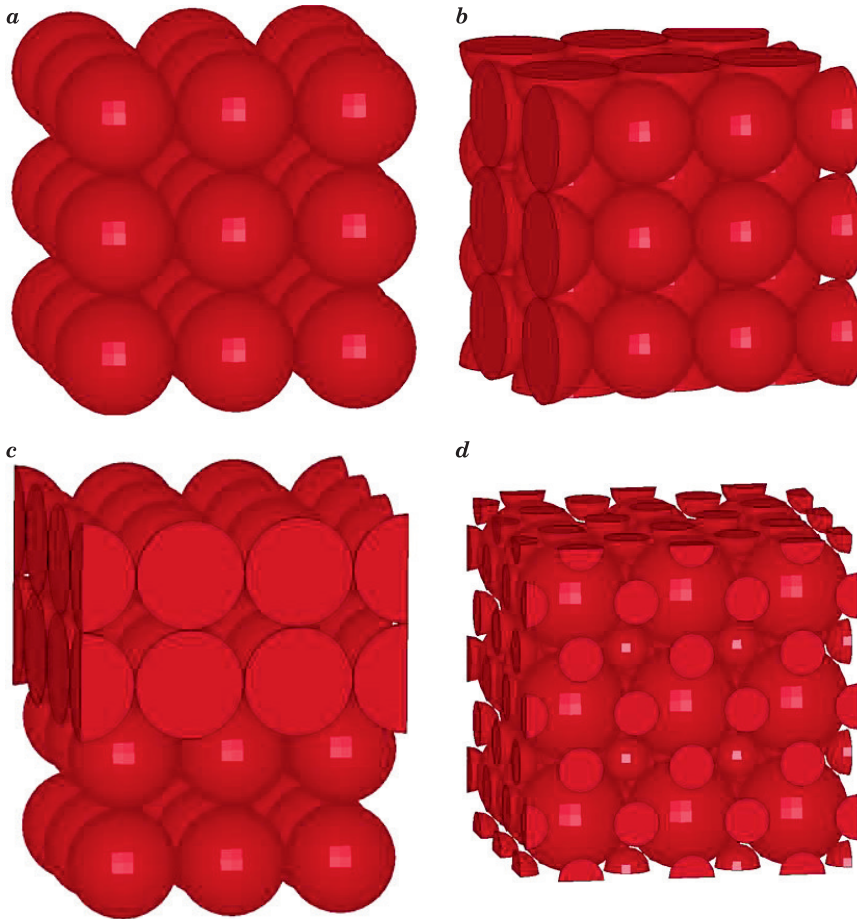


Fig. 5. Numerical models of porous ceramics microstructure: *a* – **u1**, *b* – **u2**, *c* – **u3**, *d* – **u4**

Solid hexagonal 4-nodal elements were used to developed the finite element mesh. The applied material model was \*MAT\_JOHNSON\_HOLMQUIST\_CERAMICS which is useful when modeling brittle materials, such as ceramics, subjected to large pressures, shear strain and high strain rates. The model attempts to include the phenomena encountered when brittle materials are subjected to load and damage. The equivalent stress for a ceramic-type material is given by HALLQUIST (2016):

$$\sigma^* = \sigma_i^* - D(\sigma_i^* - \sigma_f^*) \tag{13}$$

where:

$$\sigma_i^* = a(p^* + t^*)^n(1 + c \ln \epsilon^*) \tag{14}$$

represents the intact, undamaged behavior,

$$D = \sum \Delta \varepsilon^p / \varepsilon_f^p \quad (15)$$

represents the accumulated damage based upon the increase in plastic strain per computational cycle and the plastic strain to fracture:

$$\varepsilon_f^p = d_1(p^* + t^*)^{d_2} \quad (16)$$

and

$$\sigma_f^* = b(p^*)^m(1 + c \ln \dot{\varepsilon}) \leq \text{SFMAX} \quad (17)$$

represents the damaged behavior. In each case, the ‘\*’ indicates a normalized quantity, the stresses being normalized by the equivalent stress at the Hugoniot elastic limit, the pressures by the pressure at the Hugoniot elastic limit and the strain rate by the reference strain rate (HALLQUIST 2016).

The material constants for  $\text{Al}_2\text{O}_3$  were shown in Table 1.

Table 1

Material constants for $\text{Al}_2\text{O}_3$ (CRONIN at al., 2003)	
Parameter	Value
Density [ $\text{kg/m}^3$ ]	3,226
Shear Modulus [GPa]	90.16
Strength Constants	
A	0.93
B	0.31
C	0.0
M	0.6
N	0.6
Ref Strain Rate (EPSI)	1.0
Tensile Strength [GPa]	0.2
Normalized Fracture Strength	NA
HEL [GPa]	2.79
HEL Pressure [GPa]	1.46
HEL Vol. Strain	0.01117
HEL Strength [GPa]	2.0
Damage Constants	
D1	0.005
D2	1.0
Equation of State	
K1 [GPa] (Bulk Modulus)	130.95
K2 [GPa]	0
K3 [GPa]	0
Beta	1.0

The boundary conditions were as follows: the model was stated on the rigid wall, compression was carried out with the displacing rigid wall (velocity  $v = 1 \text{ mm/ms}$ ), rigid walls also blocked the rest of walls of the model to simulate

the influence of the surrounding structure. The surface to surface contact with penalty function was applied. The static friction coefficient between ceramic faces and rigid wall and ceramic was 0.3 and dynamic one – 0.2.

### Results and discussion

The results were shown as deformations in time step of 0, 0.5 and 1 ms (Fig. 6) and stress-strain curves (Fig. 7). It must be mentioned that stress was calculated on the base of initial cross-section of the polyhedron escribed on each model and reaction force in the base rigid wall. Strain was calculated on the base of initial height of the sample and displacement of the moving rigid wall.

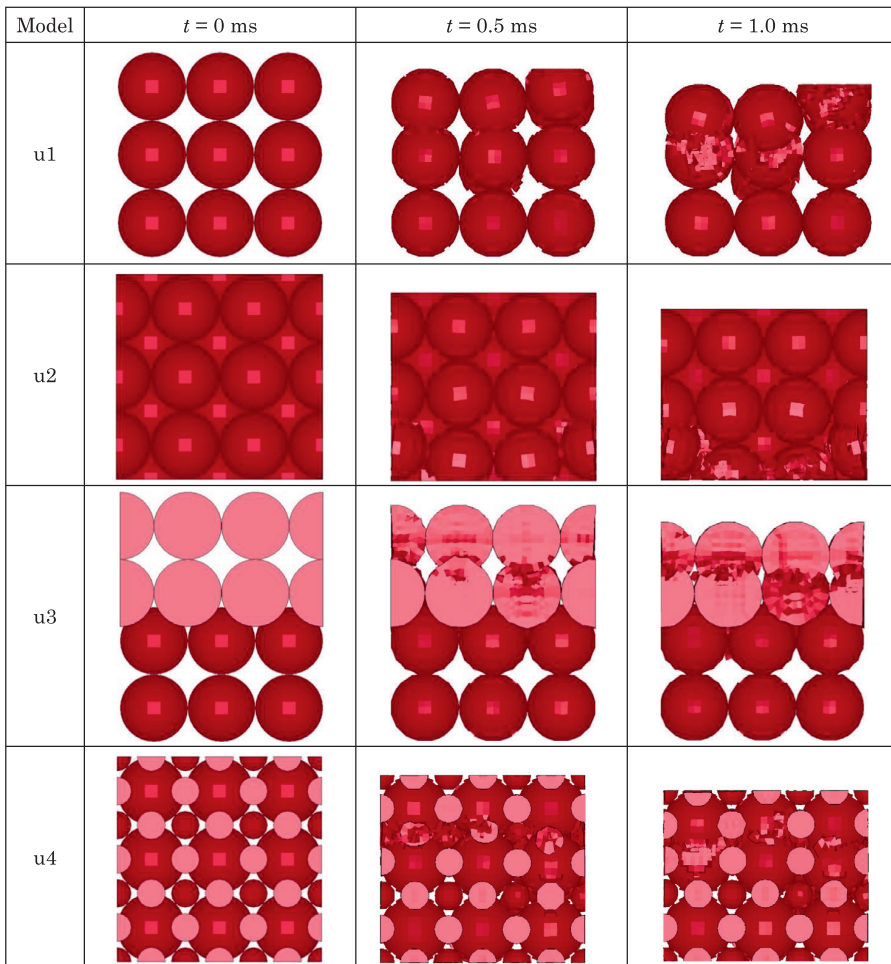


Fig. 6. Deformations of porous ceramics microstructure numerical models during compression

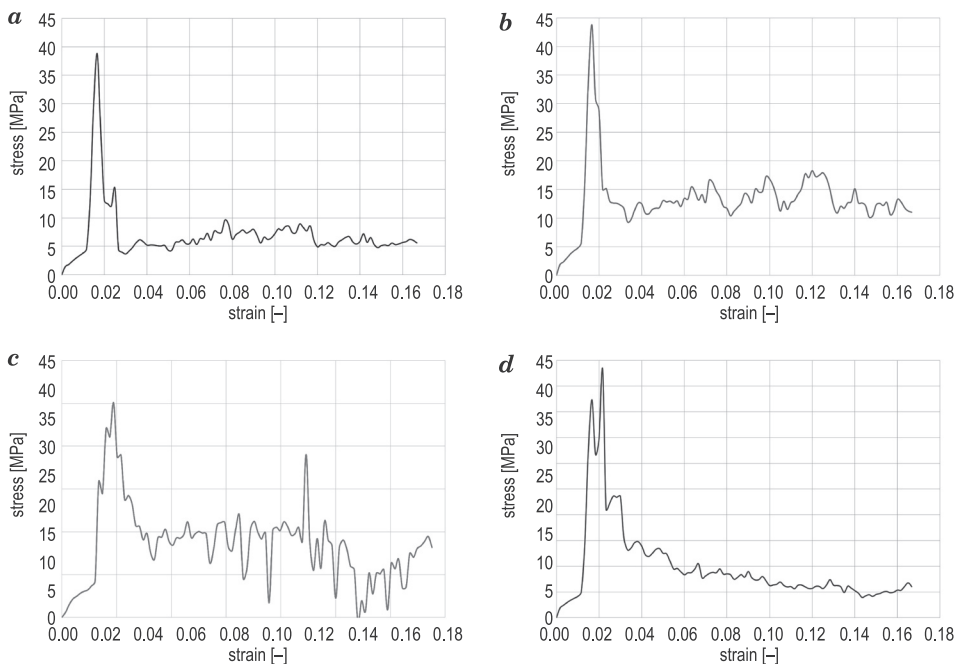


Fig. 7. Stress – strain charts for porous ceramics microstructure numerical models during compression test: *a* – **u1**, *b* – **u2**, *c* – **u3**, *d* – **u4**

To assess the differences between models the comparison stress – strain chart was prepared (Fig. 8). Also values of mass, porosity and maximum stress were compared in Figure 9.

Firstly, the differences in deformations between models were observed. They depended on the spheres distribution. For **u1** model the damage begins in the middle of the sample, in **u2** and **u4** models – at the top and in **u3** – at the bottom.

Also the stress-strain charts differed from each other. Even though the maximum stress appeared for the same strain for all samples (0.2), it must be noticed that the charts shape after that point reflected the microstructural specific behaviour for each spheres distribution. The most interesting example of this phenomenon can be seen for **u4** chart, where two “peaks” of stress appeared – what was the result of small and big spheres damage.

Comparing the maximum stress values it was visible that the biggest one was for **u4** distribution, when the smallest one – for **u3**. The biggest porosity value was for **u1** sample, the smallest one – for **u2**. Considering mass – the biggest one was for **u2** sample, the smallest one for **u1**.

However, the most important factors for assessing the porous ceramics for implementation as proppant material were maximum stress vs. porosity and maximum stress vs. mass ratios (marked as MS/P and MS/M accordingly) – shown

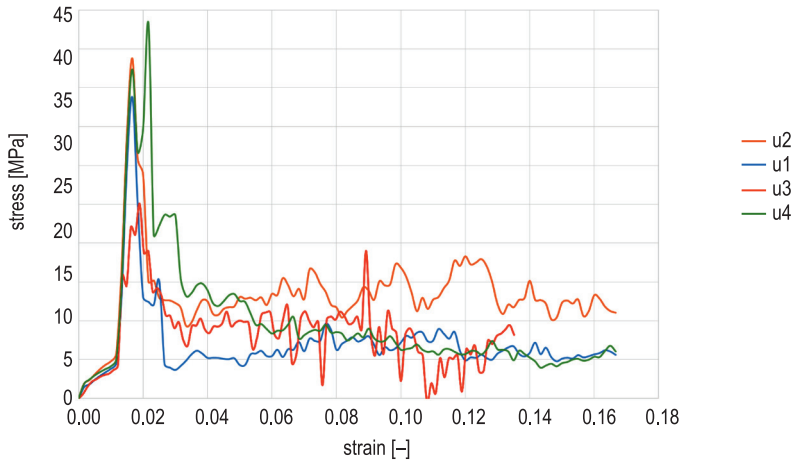


Fig. 8. Comparison of stress – strain characteristics for porous ceramics microstructure numerical models during compression test

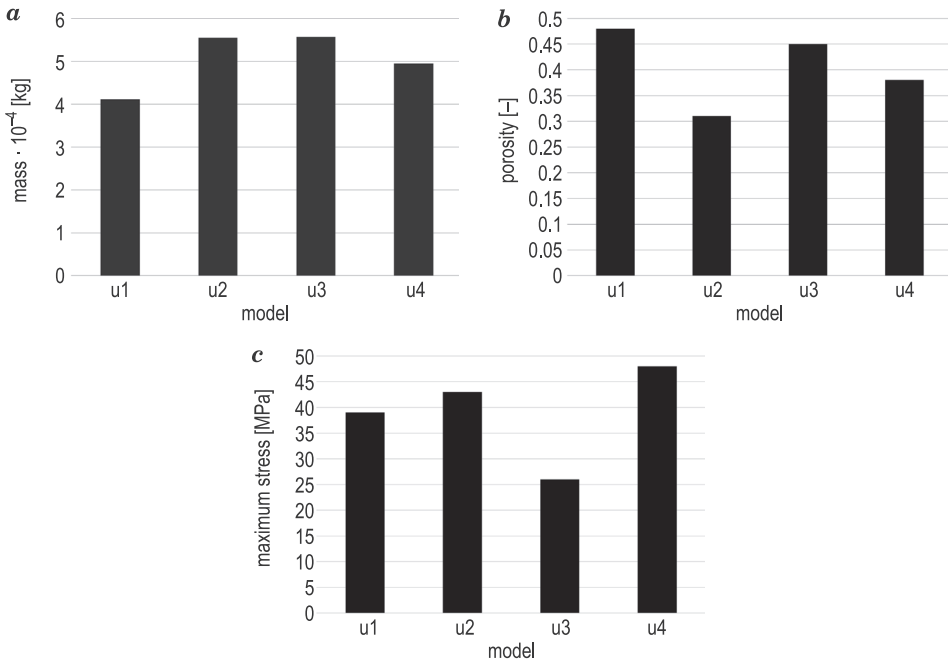


Fig. 9. Comparison of mass, porosity and maximum stress values for porous ceramics microstructure numerical models during compression test: *a* – mass – comparison, *b* – porosity – comparison, *c* – maximum stress – comparison

in Table 2. The MS/P ratio is very important considering the fracture supporting ability of proppant (should be as big as possible) and gas flow through fracture (also as big as possible). The MS/M ratio reflected the ability of proppant to support the fracture versus its mass, which can be very important for the phenomenon of carrying the proppant by the fracking fluid to the fracture (the lightest proppant is, the further it can be placed in the crack supporting the larger area of open fracture). In this case the best value of MS/P ratio (the smallest one) was observed for **u3** sample, also acceptable for **u1** one. But in the same time the **u3** and **u1** samples were characterized by the worse MS/M ratio.

Table 2

Maximum stress vs. porosity and maximum stress vs. mass ratios  
(marked as MS/P and MS/M accordingly) for tested models

Model	MS/P	MS/M
u1	79.9	9.42
u2	139.6	7.98
u3	55.6	4.57
u4	126.8	9.75

## Conclusions

The research presented in the paper was dedicated to study the influence of the grains distribution in porous ceramics on such material global mechanical properties with mass and porosity consideration. The study was carried out using finite element method and idealistic models of described structures.

On the base of achieved results it can be concluded that the selection of the porous ceramics microstructure for the implementation as proppant material should be based on the needs of the fracturing process design, which depend on e.g. shale reservoir geological properties and the depth on which it is situated. Finally, it must be mentioned that the solid ceramics has two or three times bigger compression strength but does not allow to increase the gas flow in the wellbore. So the proppant selection also should be based on the strength requirements for a fractured reservoir.

## Acknowledgements

The paper supported by a grant No BG2/DIOX4SHELL/14 financed in the years 2014-2018 by The National Centre for Research and Development, Poland.

## References

- CRONIN D.S., BUI K., KAUFMANN C., MCINTOSH G., BERSTAD T., CRONIN D. 2003. *Implementation and validation of the Johnson–Holmquist ceramic material model*. In Proceedings of LS-DYNA 4<sup>th</sup> European LS-DYNA Users Conference, UIM, Germany.
- DOLTSINIS I., DATKE R. 2001. *Modelling the damage of porous ceramics under internal pressure*. Computer Methods in Applied Mechanics and Engineering, 191(1-2): 29-46.
- HALLQUIST J. 2006. *LS-DYNA theory manual*. LSTC, Livermore.
- HAMMEL E.C., IGHODARO O.L.-R., OKOLI O.I. 2014. *Processing and properties of advanced porous ceramics: An application based review*. Ceramics International, 40(10): 15351-15370.
- KALITA S.J., BOSE S., HOSICK H.L., BANDYOPADHYAY A. 2003. *Development of controlled porosity polymer – ceramic composite scaffolds via fused deposition modelling*. Materials Science and Engineering, C, 23: 611-620.
- KNEZ D., ZIAJA J., PIWOŃSKA M. 2017. *Computer simulation of the influence of proppant high diameter grains damage on hydraulic fracturing efficiency*. AGH Drilling, Oil, Gas, 34(2): 411-418.
- LO S.-W., MILLER M.J., LI J. 2002. *Encapsulated breaker release rate at hydrostatic pressure at elevated temperatures*. In Proceedings of SPE Annual Technical Conference and Exhibition, San Antonio, Texas, SPE-77744.
- MIEDZIŃSKA D., NIEZGODA T., MAŁEK E., ZASADA Z. 2013. *Study on coal microstructure for porosity levels assessment*. Bulletin of the Polish Academy of Sciences — Technical Sciences, 61(2): 499-505.
- MURPHY B. 2013. *CARBO Ceramics is Sitting in the Fracking Catbird Seat: CRR, UPL, CHK*. SmallCap Network, 1: 13-15.
- PETTY N.A., XU G. 2010. *The Effects of Proppant Concentration on the Rheology of Slurries for Hydraulic Fracturing - A review*. UCR Undergraduate Research Journal, 1: 45-50.
- SADOWSKI T., SAMBORSKI S. 2003. *Prediction of the mechanical behaviour of porous ceramics using mesomechanical modelling*. Computational Materials Science, 28(3-4): 512-517.
- SHCHUROVA E.I. 2016. *Modeling of the Ceramics Structure for the Finite Element Analysis*. Procedia Engineering, 150: 179-184.
- STUDART A.R., GONZENBACH U.T., TERVOORT E., GAUCKLER L.J. 2006. *Processing routes to macroporous ceramics: a review*. Journal of the American Ceramic Society, 89: 1771-1789.
- WALSH D., BOANINI E., TANAKA J., MANN S. 2005. *Synthesis of tri-calcium phosphate sponges by interfacial deposition and thermal transformation of self-supporting calcium phosphate films*. Journal of Materials Chemistry, 15: 1043-1048.
- WEAVER J.D., BATENBURG D.W., NGUYEN P.D. 2007. *Fracture-Related Diagenesis May Impact Conductivity*. Petroleum Engineers Source SPE, 12(3): 155-163.

